Electronic Supplementary Material (ESI) for New Journal of Chemistry.

Supporting Information

Colorimetric chemosensor based on a Schiff base for highly selective sensing of cyanide in aqueous solution: Influence of solvents

Yu Jeong Na, Gyeong Jin Park, Hyun Yong Jo, Seul Ah Lee, Cheal Kim*

Department of Fine Chemistry and Department of Interdisciplinary Bio IT Materials, Seoul National University of Science and Technology, Seoul 139-743, Korea. Fax: +82-2-973-9149; Tel: +82-2-970-6693; E-mail:chealkim@seoultech.ac.kr

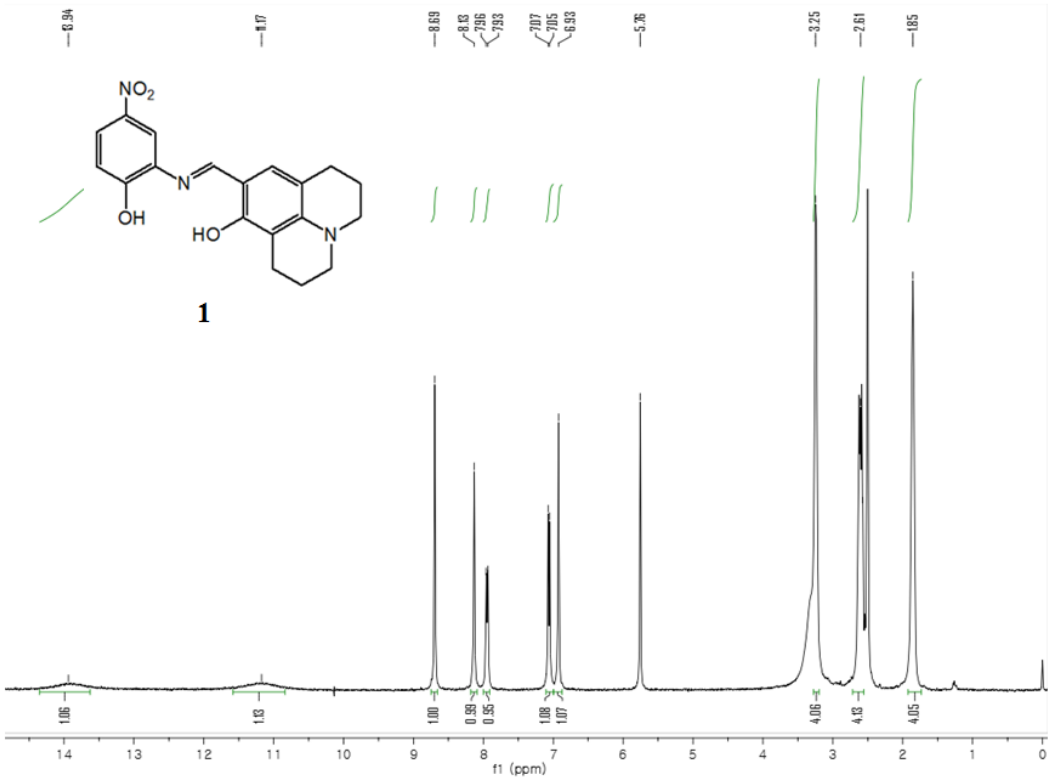

Fig. S1 ^{1}H NMR spectrum of **1**.

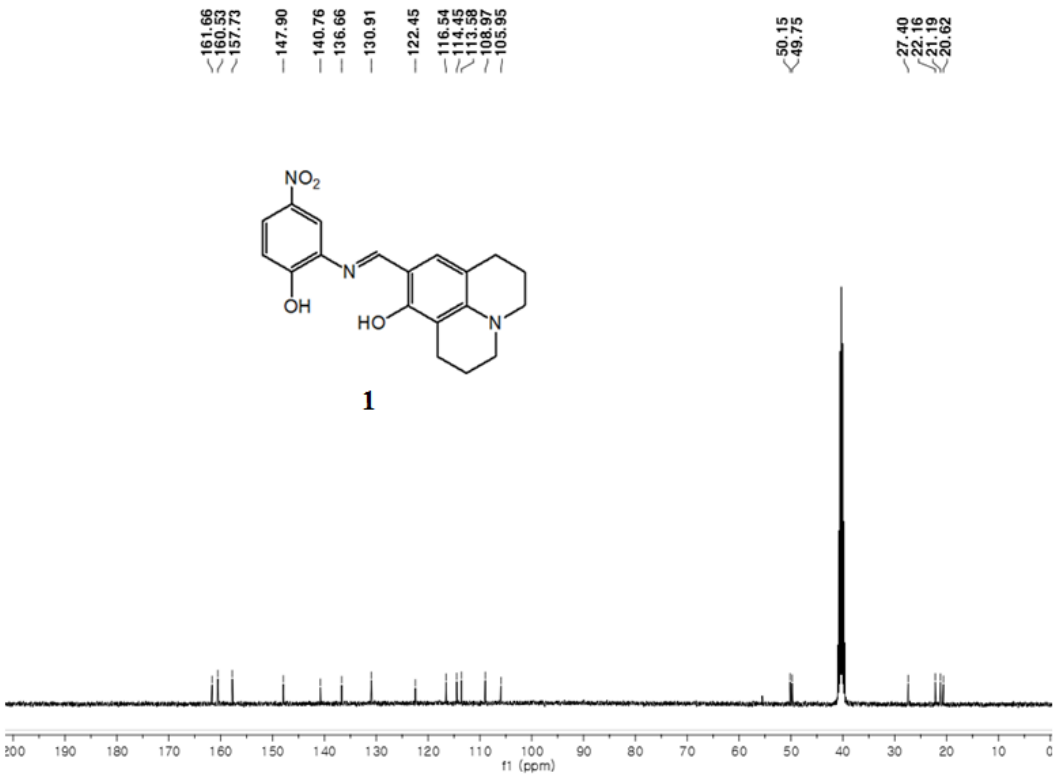

Fig. S2 ^{13}C NMR spectrum of **1**.

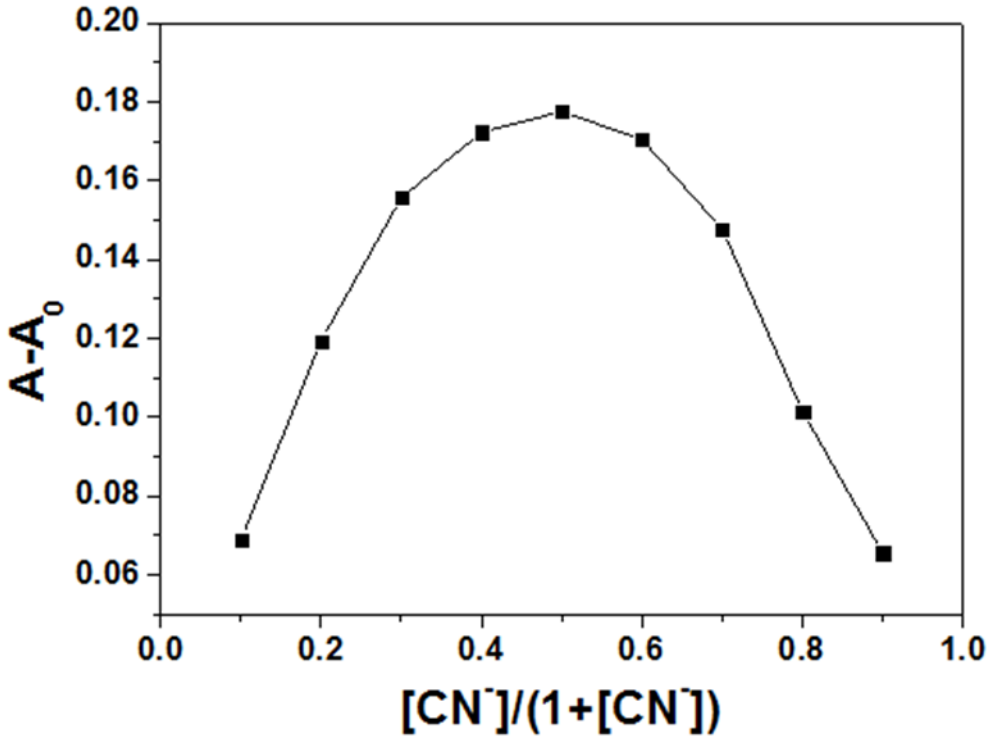

Fig. S3 Job plot of receptor **1** and cyanide in a mixture of methanol/H_2O (2:1, v/v).

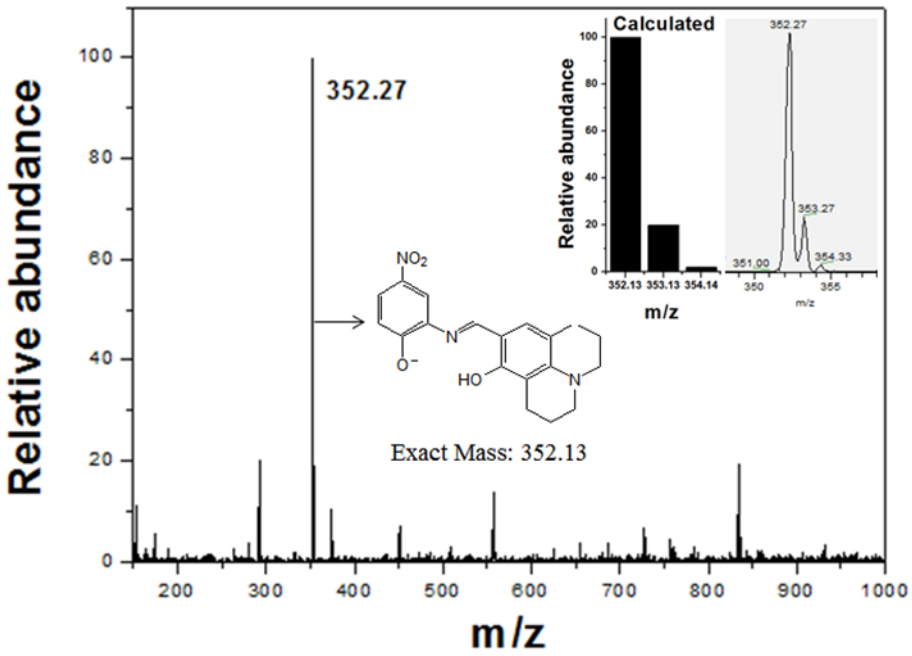

Fig. S4 Negative-ion electrospray ionization mass spectrum of **1** upon addition of 1 equiv of CN^- in a mixture of methanol/H_2O (2:1, v/v).

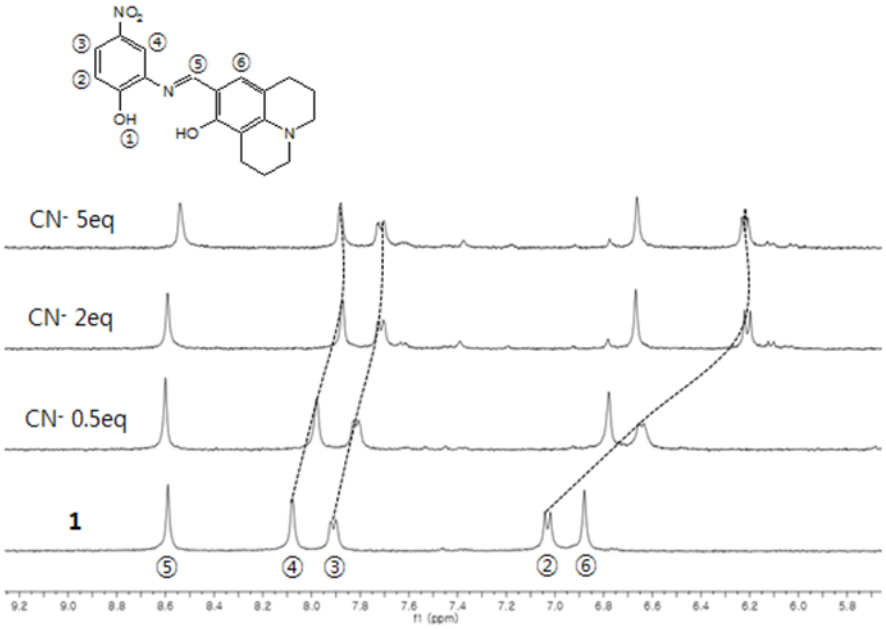

Fig. S5 ^{1}H NMR titration of **1** (10 mM) with CN^- in DMSO-d_6/CD_3OD/D_2O (5:2:1, v/v/v).

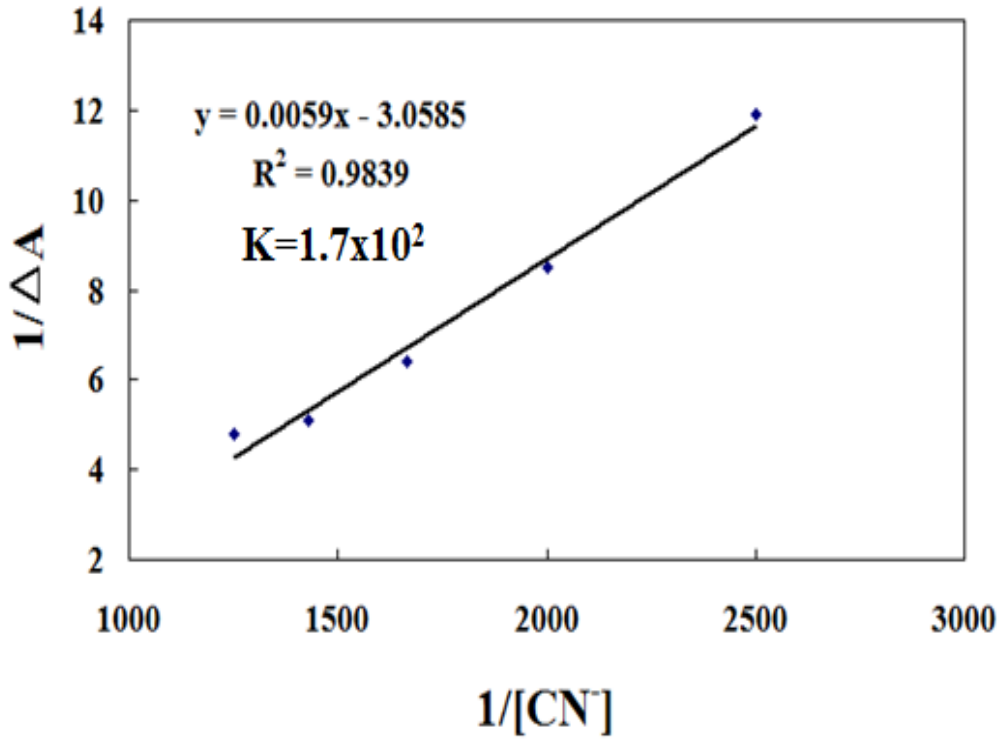

Fig. S6 Benesi-Hildebrand plot (absorbance at 479 nm) of **1**, assuming a 1:1 stoichiometry for association between **1** and CN^- in a mixture of methanol/H_2O (2:1, v/v).

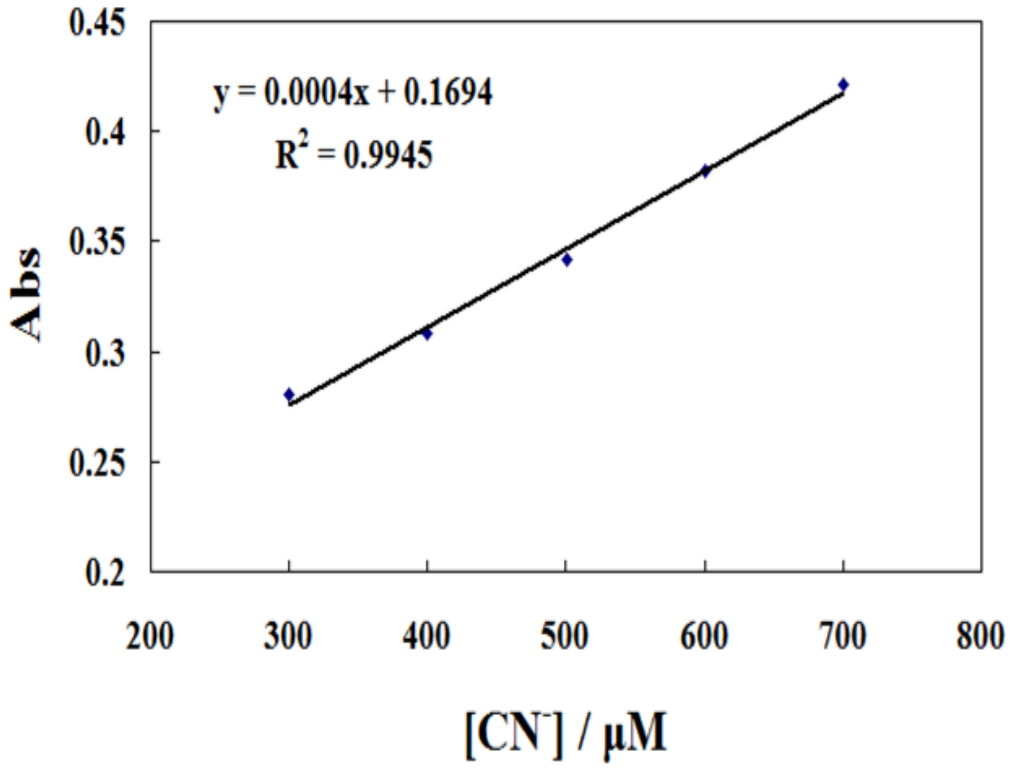

Fig. S7 Determination of the detection limit based on absorbance change (absorbance at 500 nm) of **1** (20 μM) with CN^- in a mixture of methanol/H_2O (2:1, v/v).

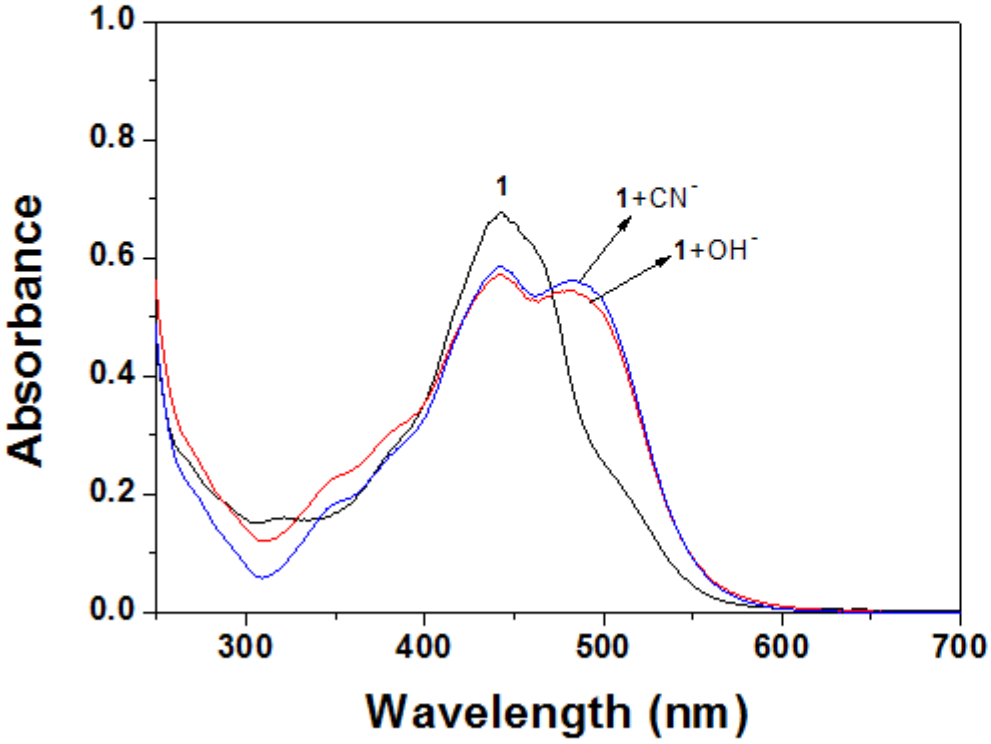

Fig. S8 Changes in the UV-vis spectra of receptor **1** upon addition of CN^- and OH^-, respectively, in a mixture of methanol/H_2O (2:1, v/v).

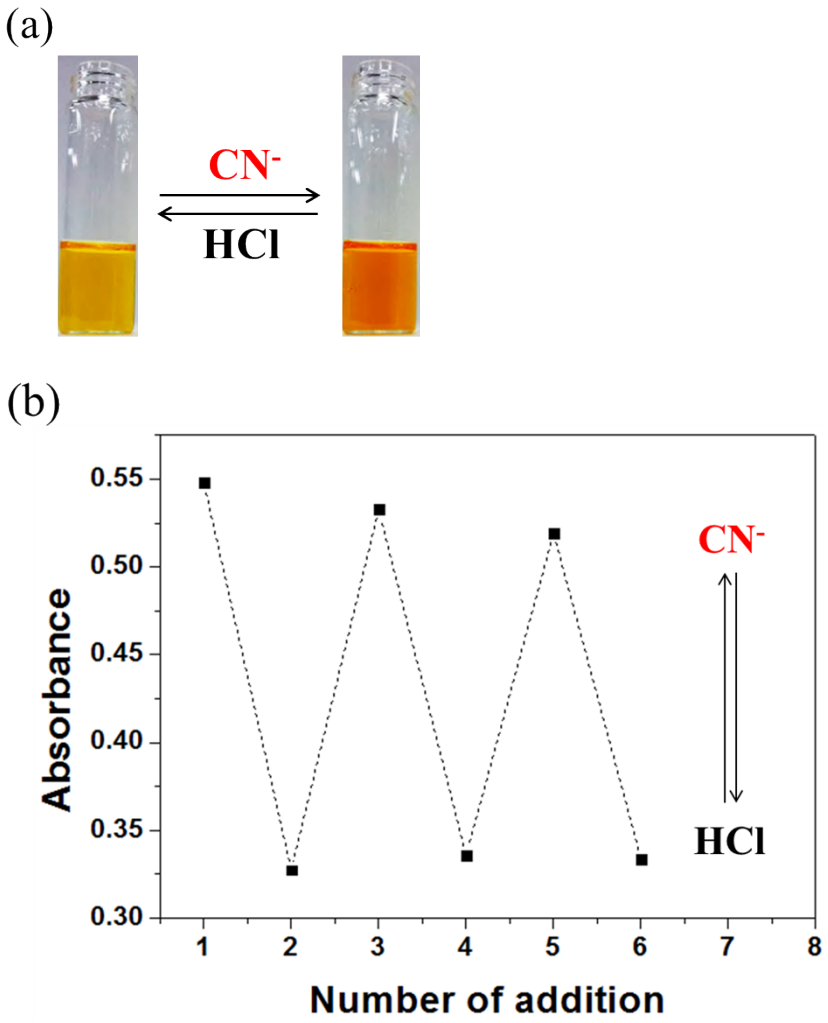

Fig. S9 (a) Colorimetric changes of **1** (20 μM) after the sequential addition of CN^- and HCl in a mixture of methanol/H_2O (2:1, v/v). (b) Reversible changes in absorbance of **1** (20 μM) at 500 nm after the sequential addition of CN^- and HCl.

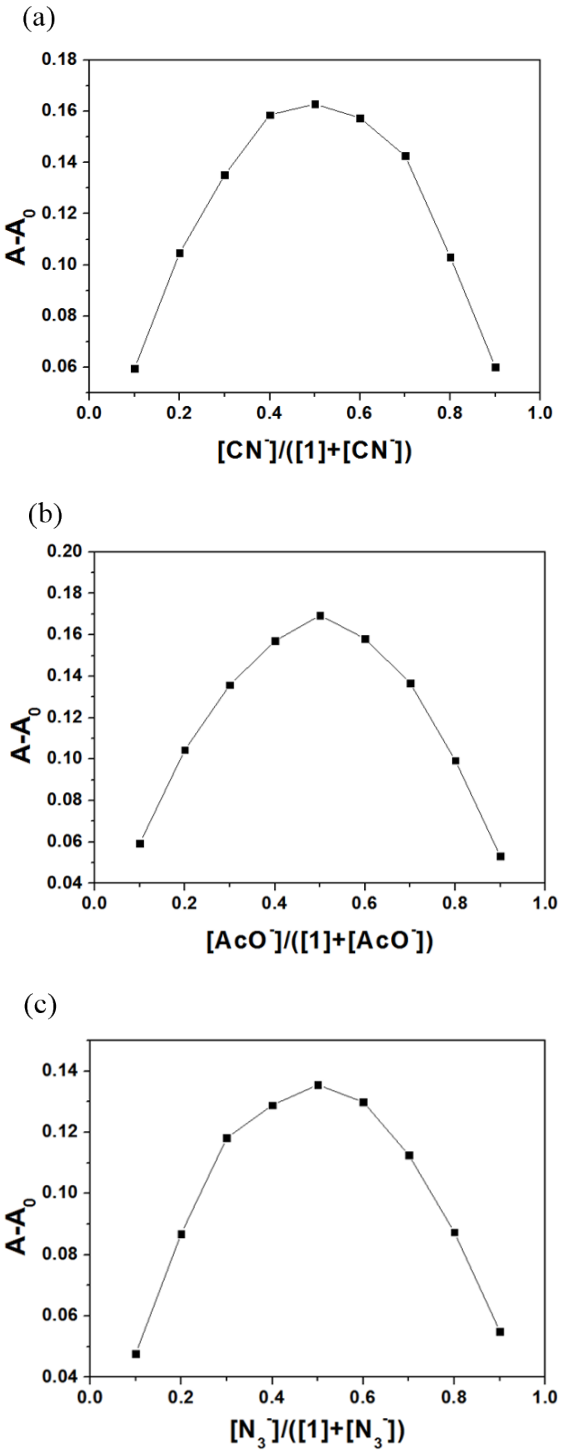

Fig. S10 Job plots of receptor **1** with (a) CN^-, (b) AcO^-, and (c) N_3^- in methanol.

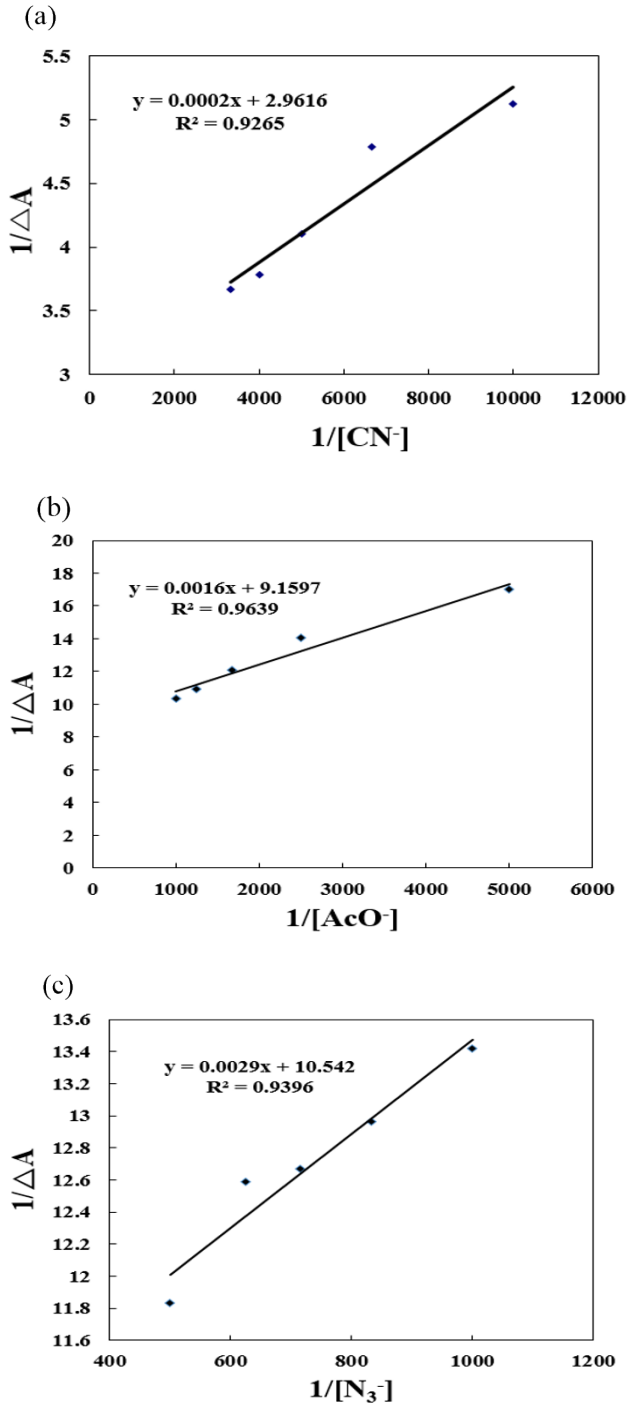

Fig. S11 Benesi-Hildebrand plots (absorbance at 500 nm) of **1**, assuming a 1:1 stoichiometry for association between **1** and (a) CN^-, (b) AcO^-, (c) N_3^- in methanol.

(a)

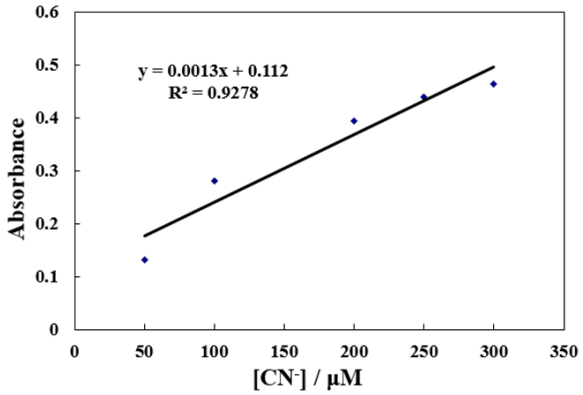

(b)

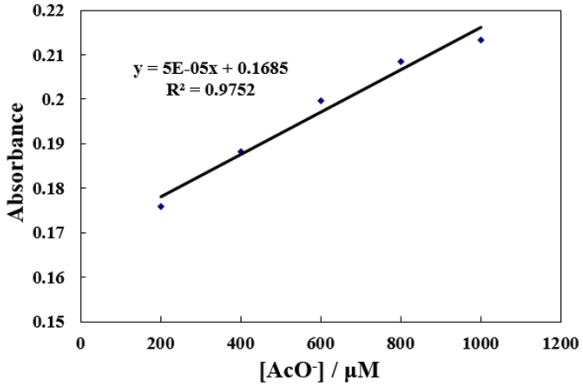

(c)

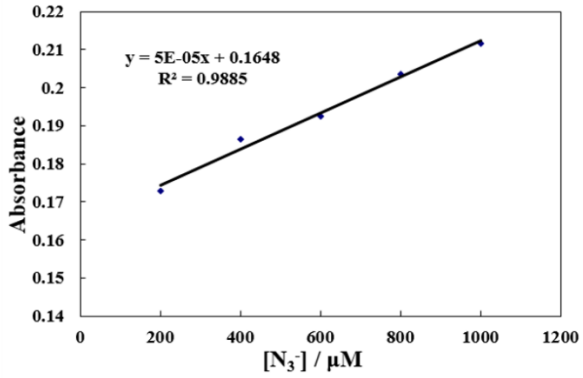

Fig. S12 Determination of the detection limit based on absorbance change (absorbance at 500 nm) of **1** (20 μM) with (a) CN^-, (b) AcO^-, and (c) N_3^- in methanol.

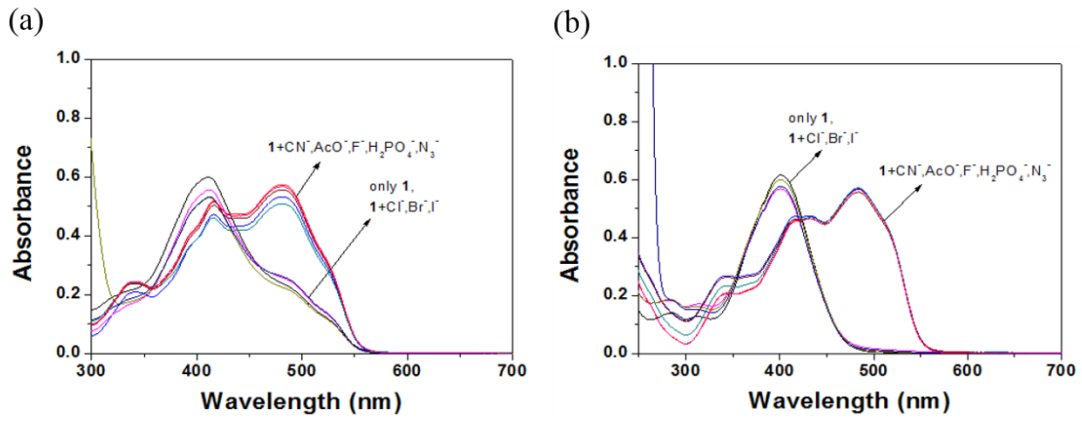

Fig. S13 (a) UV-vis spectral changes of **1** (20 μM) upon the addition of various anions (40 equiv) in DMF. (b) UV-vis spectral changes of **1** (20 μM) upon the addition of various anions (40 equiv) in acetonitrile.

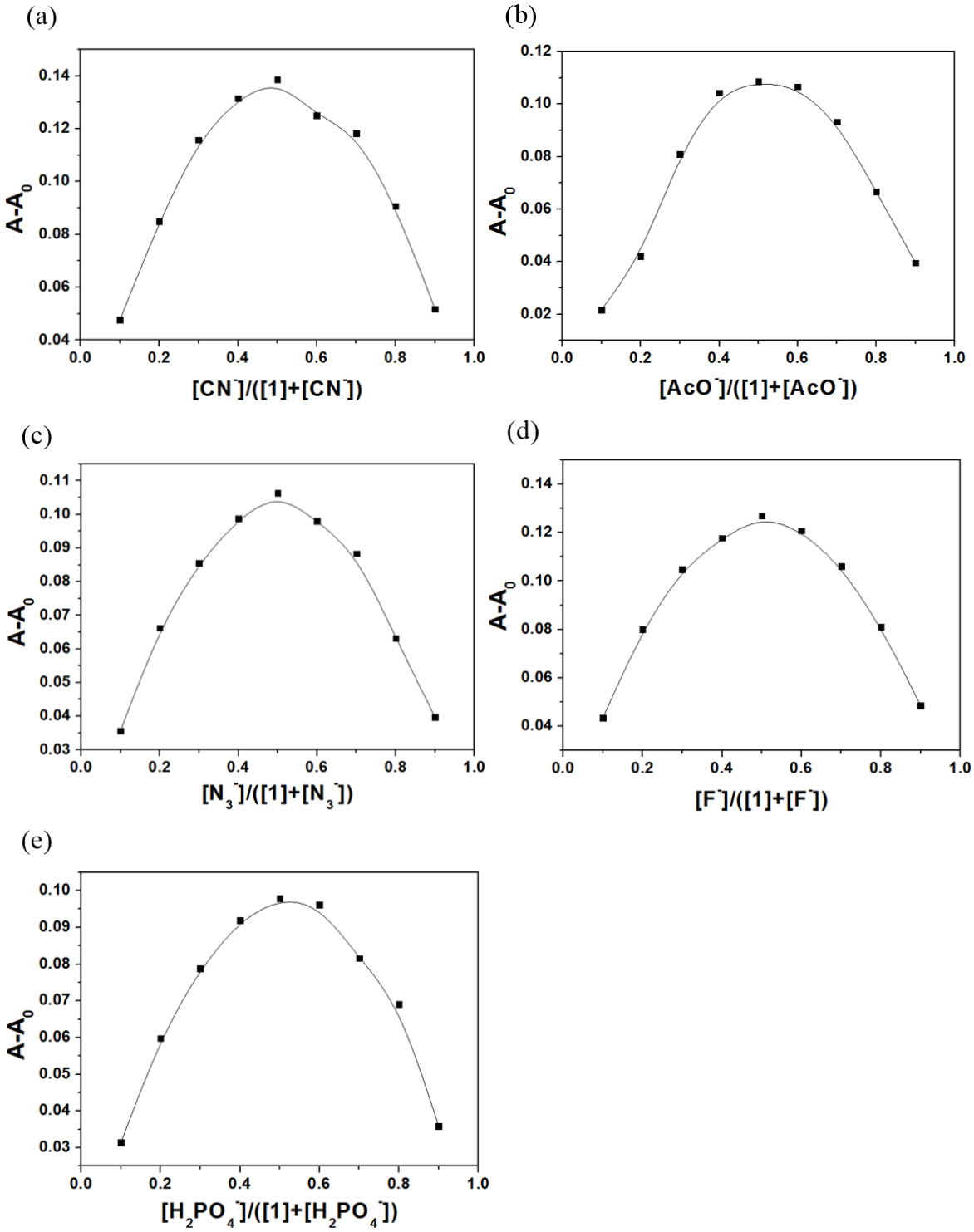

Fig. S14 Job plots of receptor **1** with (a) CN^-, (b) AcO^-, (c) N_3^-, (d) F^-, and (e) $H_2PO_4^-$ in DMSO.

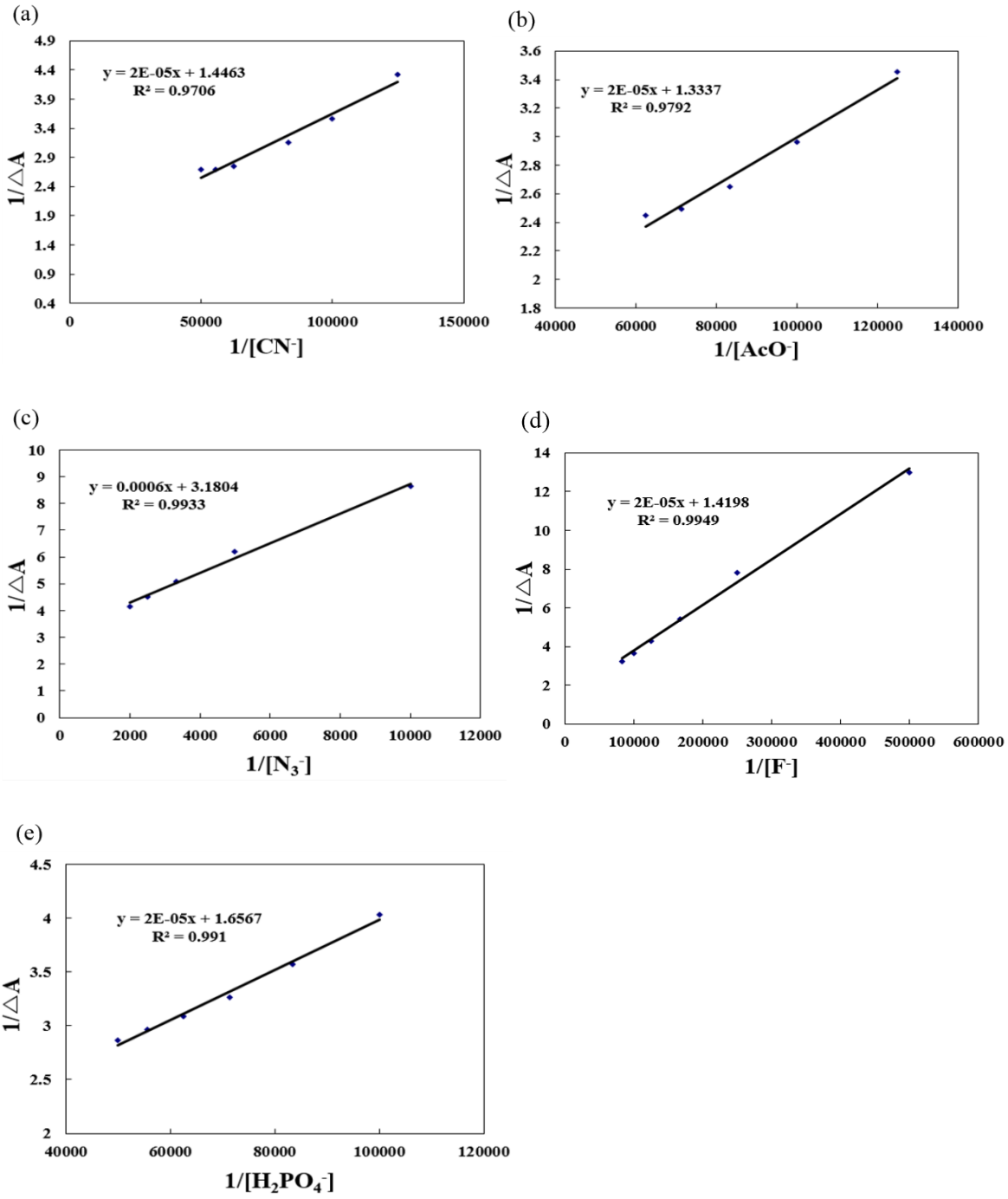

Fig. S15 Benesi-Hildebrand plots (absorbance at 500 nm) of **1**, assuming a 1:1 stoichiometry for association between **1** and (a) CN^-, (b) AcO^-, (c) N_3^-, (d) F^-, (e) $H_2PO_4^-$ in DMSO.

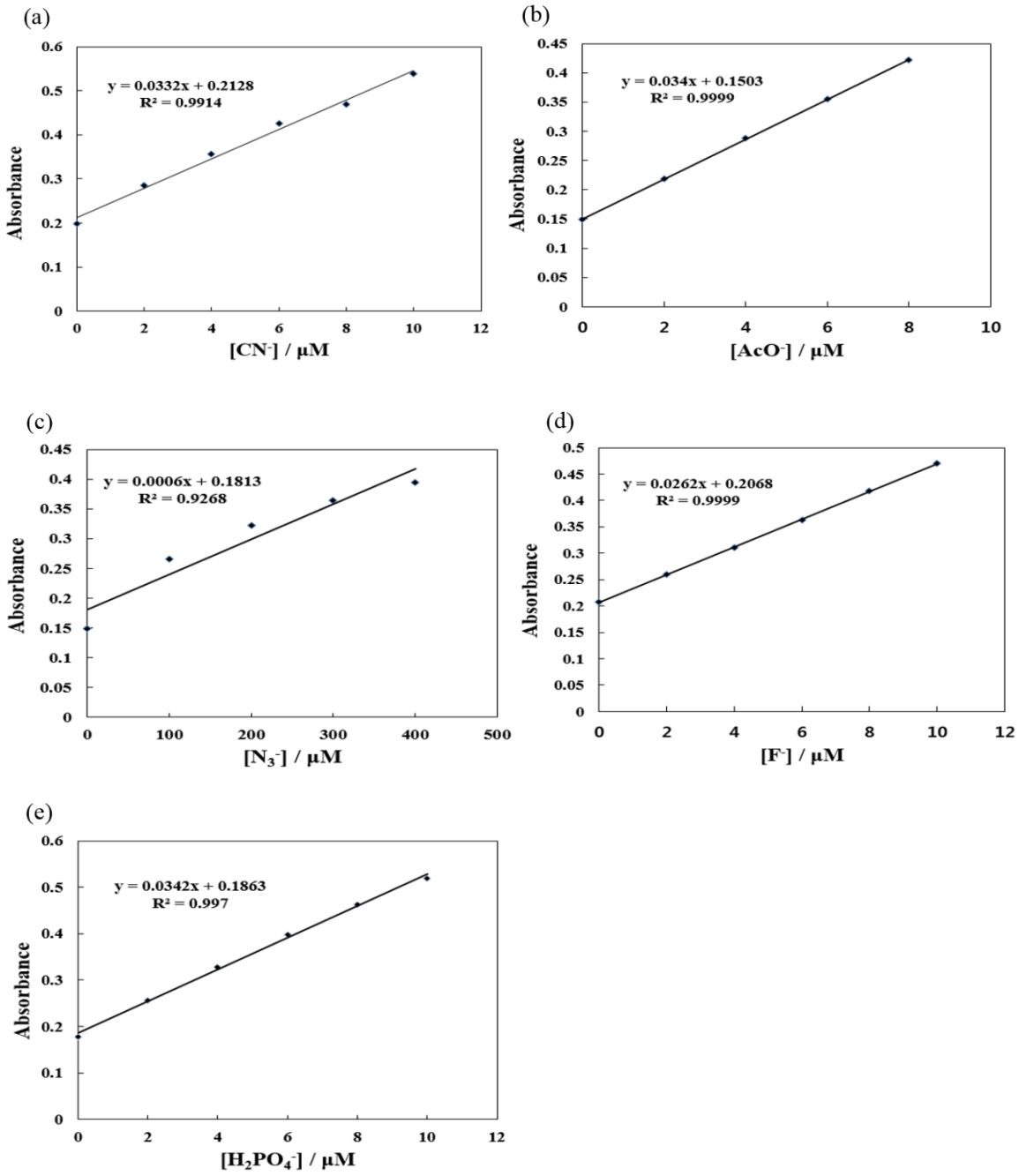

Fig. S16 Determination of the detection limit based on intensity change (absorbance at 500 nm) of **1** (20 μM) (a) with CN^-, (b) AcO^-, (c) N_3^-, (d) F^-, and (e) $H_2PO_4^-$ in DMSO.